RSC Advances

ROYAL SOCIETY OF CHEMISTRY

www.rsc.org/advances

Electrochemical detection of mercury using biosynthesized hydroxyapatite nanoparticles modified glassy carbon electrode without preconcentration

P. Kanchana[1], N. Sudhan[1], S. Anandhakumar[2], J. Mathiyarasu[2], P. Manisankar[3], C. Sekar[1*]

[1]Department of Bioelectronics and Biosensors, Alagappa University, Karaikudi-630 004, Tamilnadu, India.

[2]Central Electrochemical Research Institute, Karaikudi-630 006, Tamilnadu, India.

[3]Department of Industrial Chemistry, Alagappa University, Karaikudi-630 003, Tamilnadu, India.

Abstract

An electrochemical method for the determination of trace levels of mercury (II) ions using hydroxyapatite (HA) nanoparticles modified glassy carbon electrode (GCE) by square wave voltammetry is described for the first time. HA nanoparticles biosynthesized using *Aloe vera* plant (Av) extract exhibited improved electrocatalytic activity towards Hg^{2+} ions when compared to pristine HA. The Av-HA modified GCE showed an excellent selectivity and improved sensitivity towards the detection of Hg^{2+} without requiring preconcentration of mercury during voltammetric detection. Operational parameters such as pH, supporting electrolyte and scanning potential range were optimized. Under the optimum experimental conditions, the anodic peak current is proportional to the concentrations of mercury over a wide range of 2.0×10^{-7} to 2.1×10^{-4} M with the lowest detectable concentration of 141 nM. The Av-HA modified GCE showed good selectivity towards mercury in the presence of potential interferents such as copper, lead, cadmium, silver and zinc. The fabricated sensor displayed good reproducibility and is suitable for the determination of mercury in tap water and industry waste water.

***Keywords*:** Hydroxyapatite, mercury sensor, *Aloe vera*, square wave voltammetry

*Corresponding author: Dr. C. Sekar, Department of Bioelectronics and Biosensors.
Tel.: +91 9442563637, E-mail: Sekar2025@gmail.com

1. Introduction

Heavy metals are major contributors to the environmental pollution because of their involvement in many natural and industrial processes. Mercury and its compounds are highly toxic, even at trace levels, when they accumulate in vital organs such as liver, heart muscle, brain, etc., and can cause kidney injury, central nervous system disorders and even death [1, 2]. For these reasons, there is an increasing need for quantification of mercury in the environment, foodstuff and pharmaceutical products. Electroanalysis is one of the most favourable techniques for the determination of heavy metal ions because of its low cost, high sensitivity and easy operation. Chemically modified electrodes have been intensively used in electrochemical analysis due to their high sensitivity and excellent selectivity. To date, numerous modified electrodes have been developed for the determination of mercury which include gold-poly(3,4-ethylenedioxythiophene [3], chitosan modified electrode [4], multi-walled carbon nanotubes [5], gold nanoparticle [6], α-MnO_2 nanocrystals [7] and α- and β-cyclodextrins [8]. Among these, gold was found to be the superior choice of electrode material owing to its high affinity towards mercury that enhance the sensitivity [9]. However, the major setback of gold electrodes is the structural changes on the electrode surface, caused by amalgam formation [10] that necessitates complex electrochemical and mechanical treatment to achieve reproducibility [11]. Hence, low cost material preparation and simple electrode modification method continued to be an important topic of research for determination of mercury with improved sensitivity, selectivity and reproducibility.

Hydroxyapatite ($Ca_{10}(PO_4)_6(OH)_2$, HA) is the main mineral constituent of natural bone and teeth. It attracts considerable interest in many areas because of its acid-base properties, ion-exchange ability, biocompatibility and adsorption capacity. A great variety of cationic and anionic substitutions in HA is possible due to its "open structure'' [12, 13]. In our earlier studies, we have demonstrated the applicability of HA based electrodes for the

determination of tyrosine, uric acid and folic acid [14-16]. The hydroxyapatite NPs modified GCE have been proved to be highly sensitive and reliable for the detection of the chosen analytes. The characteristics of HA NPs depend on the method of synthesis which influences particle size, shapes and phase purity. A number of novel processing routes such as dry, wet, hydrothermal, sonochemical, and microwave assisted process have been developed for preparing HA powders [17]. Organic modifiers are used for the morphology and size controlled synthesis of HA (e.g. citric acid, ethylenediamminetetraacetic acid, cetyltrimethylammoniumbromide, ethylene glycol, mixed tween-80 and polyoxyethylene). Although chemical method may successfully produce pure, well-defined nanoparticles, these are quite expensive and potentially dangerous to the environment. On the other hand, biosynthetic methods employing either biological microorganisms or plant extracts are simple and eco-friendly. *Aloe vera* (*Aloe barbadensis Miller*) is a perennial succulent belonging to the Liliaceal family, and it is a cactus-like plant. The chemical composition of aloe plants is largely dependent on the species analyzed. *Aloe vera* filet contains mainly water (98.5% to 99.5%) and the remaining 0.5–1% solid material consists of a range of compounds including water and fat-soluble vitamins, minerals, enzymes, polysaccharides, phenolic compounds and organic acids [18]. This plant has been used in many medicinal applications as a result of its antipyretic, antioxidative and cathartic properties [19].

In this work, we report the biological synthesis of crystalline HA NPs by microwave irradiation method using '*Aloe vera* plant' extract. These Av-HA NPs modified glassy carbon electrodes provide a well-defined platform for the determination of Hg^{2+}. The fabricated sensor exhibits low detection limit, rapid response, excellent reproducibility, extreme simplicity and was successfully applied for the study of real sample.

2. Experimental procedure

2.1 Reagents and apparatus

Calcium nitrate ($Ca(NO_3)_2 \cdot 4H_2O$), diammonium hydrogen orthophosphate ($(NH_4)_2HPO_4$), mercury chloride ($HgCl_2$), hydrochloric acid (HCl), disodium hydrogen phosphate (Na_2HPO_4), sodium dihydrogen phosphate (NaH_2PO_4), sodium acetate trihydrate, ($CH_3COONa.3H_2O$), acetic acid ($C_2H_4O_2$) and potassium nitrate (KNO_3) purchased from Merck, Mumbai and *Aloe vera* plant extract were used as the starting materials. All the chemicals were of analytical reagent (AR) grade and used without further purification. 0.2 M potassium nitrate solution of pH 3.0 served as the background electrolyte. The deionized water used in all experiments was produced by ultra purification system and the experiments were carried out at ambient temperature.

Crystal structure and morphology of HA were characterized by powder X-ray diffraction (XRD, Rigaku X-ray diffractometer with Cu Kα of 1.5406 Å), and field emission scanning electron microscopy with energy dispersive X-ray spectroscopy (FESEM-EDX, FEG QUANTA 250) and transmission electron microscopy (TEM, Philips CM200). Fourier transform infrared (FT-IR) spectra were recorded at room temperature with an FT-IR spectrometer (Thermo Scientific Systems, Nicolet-6700) using the KBr pellet technique. Thermogravimetric (TG) analysis of the synthesized powder was performed in a SDT Q600 VB.3 Build101 instrument between 20-1000°C in air at heating rate of 20°C/min. Electrochemical measurements were carried out on CHI 609D electrochemical workstation (CH Instruments, Austin, USA). A three-electrode cell was used with a modified glassy carbon electrode (GCE) as the working electrode, Ag/AgCl as the reference electrode, and a platinum wire electrode as the counter. Electrochemical impedance spectroscopy (EIS) measurements were made by applying ac potential of amplitude 5 mV over the dc potential of 250 mV in the frequency range 100 kHz to 1 Hz in 1M KCl containing 1.0 mM $[Fe(CN)_6]^{3-/4-}$

redox couple. The impedance data are presented in the form of Nyquist plots. The value of the charge transfer resistance (R_{ct}) was determined using Zsimpwin software simulations. Cyclic voltammograms (CVs) were recorded between a potential window of -0.8 V and 0.6 V at a scan rate of 50 mVs^{-1} in 0.2 M KNO_3 containing 20 $x10^{-6}$ M $HgCl_2$. Square wave voltammetry (SWV) measurements were performed in the potential region from -0.8 to 0.6 V in 0.2 M KNO_3 (pH 3.0) with the amplitude of 50 mV, frequency 10 Hz and a step potential of 0.05 V.

2.2 Preparation of hydroxyapatite (HA) nanoparticles

Aloe vera extract was prepared from a 70 g portion of thoroughly washed *Aloe vera* leaves which were finely cut and boiled in 200 ml of deionised water. The greenish coloured *Aloe vera* extract was used as solvent (instead of deionised water) for preparing HA. In order to maintain the molar ratio of Ca/P as 1.67, 100 mL of 0.4 M $(CaNO_3)_2.4H_2O$ solution (A) and 100 mL of 0.24 M $(NH_4)_2HPO_4$ solution (B) were prepared using *Aloe vera* extract. Subsequently, solution B was added to solution A slowly with constant stirring. During the reaction, pH of the solution was maintained at 10 using ammonia solution. The mixture was then exposed to microwave irradiation of 600 W for 20 minutes (domestic microwave oven, Samsung-CE104VD, 6 power levels, 2450 MHz with input voltage of 230 V-50 Hz AC), washed with deionized water and dried at 80°C in a hot air oven and the resultant product was pale pink colour. For comparison, we synthesis pristine hydroxyapatite nanoparticle by above same procedure using deionized water, the resultant powder is white in colour. Hereafter, the HA samples prepared in deionized water and *Aloe vera* extract will be referred as HA and Av-HA respectively. Pristine hydroxyapatite was prepared repeatedly by using a microwave method and results are discussed in supplementary information (Fig. S1 and Table S1). These results indicate that the HA prepared by domestic microwave oven with the power 600 W has better reproducibility.

2.3 Electrode preparation and modification

Prior to modification, the glassy carbon electrode (GCE, 3 mm in diameter) was polished with 0.05μm alumina powder on polishing cloth, rinsed thoroughly with deionised water between each polishing step, sonicated and dried at room temperature. The modified electrodes were prepared by a simple drop casting method. HA nanoparticles were dispersed into deionized water (5 mg/mL) by ultrasonicating for about 30 min to get a stable and uniform suspension. Typically, 10 μL of HA nanoparticle suspension was drop casted onto the GCE and allowed to evaporate water at room temperature in air.

3. Results and discussion

3.1 Characterization of synthesized powders

Powder X-ray diffraction pattern of the as-synthesized pristine HA and Av-HA powders are presented in Fig. 1A. The XRD patterns are in good agreement with those of the standard HA crystallites (ICDD PDF Card No-09-432, hexagonal phase, space group $P6_3/m$). There are no characteristic peaks corresponding to impurities, such as calcium hydroxide and other calcium phosphates which implies that the phase pure HA could be prepared without requiring any high temperature treatment. Broader diffraction peaks were observed for the HA synthesized using *Aloe vera* extract indicating that the resultant HA has smaller particle size. The average crystallite size of HA and Av-HA was estimated as 18.7 nm and 9.9 nm respectively using Scherrer's equation (i.e. $D = K\lambda/\beta \cos\theta$, where K is the shape factor (0.9), β is the full width at half-maximum of diffraction peaks measured in radians, λ is the wavelength of the X-rays ($\lambda = 1.5406$ Å) and θ is the Bragg's diffraction angle).

Fig. 1B shows the FTIR spectra of HA and Av-HA samples. All the functional groups corresponding to HA are clearly observed in both HA and Av-HA samples. Two absorption bands located at 570 and 598 cm^{-1} are ascribed to the ν_4 bending mode of PO_4^{3-}. The

stretching vibration band of OH^- is observed at 628 and 3568 cm^{-1}. The band at 958 cm^{-1} is also related to the ν_1 stretching mode of PO_4^{3-}. The characteristic bands observed at 1035 and 1098 cm^{-1} are assigned to the ν_3 stretching vibration of PO_4^{3-}. The peaks found at 3446 and 1634 cm^{-1} are attributed to the ν_2 bending mode of adsorbed water [20]. In both the pristine HA and Av-HA, the carbonate peak with nearly equal intensity appeared at ~1390 cm^{-1} which could be attributed to the CO_3^{2-} group because of CO_2 adsorbed from atmosphere during synthesis process. Specifically, the peak intensities corresponding to various functional groups in the Av-HA were found to be smaller than those of pristine HA. A broadened absorption band at 1614 cm^{-1} is due to the amide group vibration of protein/enzymes in *Aloe vera* extract [21]. Another broad band at 1384 cm^{-1} corresponds to vibration of C=C stretching of aromatic amine group present in *Aloe vera* extract. Further, an intense broad absorbance band at 3320 cm^{-1} is characteristic of the hydroxyl functional group in alcohols and phenolic compounds present in *Aloe vera* extract [19].

<Fig. 1>

Fig. 2 shows FE-SEM micrographs and EDX spectra of the pristine HA and Av-HA samples. The HA crystallizes in the form of layered platelets, whereas, *Aloe vera* assisted HA form as near spherical shaped agglomerates as shown in Figs. 2a&b respectively. The long chain polysaccharides present in *Aloe vera* extract seem to affect the homogeneous distribution of HA crystallites leading to spherical agglomeration of tiny crystals. Further, TEM analysis of Av-HA clearly indicate the presence of HA nanparticles in the bulk spherical agglomerate as can be seen in Fig. 3. The EDX results show that the HA and Av-HA are primarily composed of Ca, P, and O with the Ca/P ratio of 1.60 for HA and 1.66 for Av-HA which are very close to the stochiometric value of HA (Ca/P = 1.67).

<Fig. 2>

<Fig. 3>

Thermal analyses of both the pristine HA and Av-HA were carried out in order to understand the role of *Aloe vera* extract on the crystallization of HA and to assess the quantity of residues present in the Av-HA NPs. Thermogravimetric (TG) curves were recorded on powdered HA and Av-HA between 20-1000°C in air at a heating rate of 20°C/min (Fig. 4). The initial weight loss up to 200 °C is significantly higher for the Av-HA when compared to that of pristine HA which could be attributed to the removal of weakly entrapped water, polysaccharides and aldehydes present in the *Aloe vera* extract. Subsequently, there is a weight loss of 6 % and 7% for HA and Av-HA respectively between 230 and 470 °C, which are assigned to the removal of nitrate, ammonium and other organic residuals in the raw materials. Further HA and Av-HA samples did not show any apparent weight loss in the range 400-1000°C and the final weight loss observed for HA and Av-HA were 16% and 14% respectively. Notably Av-HA sample shows lesser total weight loss when compared to the pristine HA samples. This indicated the higher thermal stability of the AV-HA samples which could partly be attributed to its smaller particle size.

<Fig. 4>

3.2 Electrochemical impedance spectroscopy (EIS) and cyclic voltammetry (CV) studies

The charge transport process of the HA and Av-HA modified GCE was studied by monitoring charge transfer resistance (R_{ct}) at the electrode/electrolyte interface. Fig. S2A shows the impedance data obtained for bare GC, HA and Av-HA modified GCE in 1 M KCl containing 1 mM of $[Fe(CN)_6]^{3-/4-}$ at scanning frequencies from 0.1 to 100 kHz. The R_{ct} value was obtained by Randles equivalent circuit [R_S (Q_{CPE} (R_{ct} W)], where R_S is the solution resistance, W is the Warburg impedance and Q_{CPE} is the constant phase element (CPE). The R_{ct} values for bare GCE (curve a), pristine HA (curve b) and Av-HA (curve c) modified GCE have been estimated as 180, 685 and 592 Ω/cm^2 respectively. It can be noticed that the R_{ct} value of Av-HA is lower than that of the HA.

The cyclic voltammograms (CVs) recorded at 50 mVs^{-1} for (a) bare GCE, (b) HA and (c) Av-HA modified electrodes in 1 M KCl containing 1 mM of $[Fe(CN)_6]^{3-/4-}$ are shown in Fig. S2B. The peak current (i_{pa}) values of bare GCE, HA and Av-HA modified electrodes were observed as 28.1 µA, 23.4 µA and 27.5 µA respectively. The Av-HA modified GCE has higher i_{pa} value when compared to pristine HA modified electrode. In addition, a significant shift in the peak potential towards less positive side can be observed for Av-HA modified GCE when compared to that of bare GCE and HA-GCE indicating fast electron transfer and improved electrocatalytic behaviour of Av-HA. The surface concentration of the HA NPs has been estimated from the plot of current versus potential (CV) using Brown–Anson model that is based on the following equation:

$$Ip = n^2F^2 I^*AV/4RT$$

where n is the number of electrons transferred, F is the Faraday constant (96,485 C mol^{-1}), I^* is the surface concentration (mol cm^{-2}), A is the surface area of the electrode (0.07 cm^2), V is the scan rate (50 mV s^{-1}), R is the gas constant (8.314 J mol^{-1} K^{-1}) and T is the absolute temperature (298 K). The value of the surface concentration of the HA and Av-HA modified electrodes has been estimated to be 7.217×10^{-9} and 8.550×10^{-9} mol cm^{-2} respectively. The observed increase in surface concentration of Av-HA is attributed to its reduced particle size when compared to that of pristine HA.

3.3 Electrochemical behaviour of mercury at Av-HA/GCE

Fig. 5A shows the cyclic voltammetric behavior of mercury (Hg^{2+}) obtained in 0.2 M KNO_3 (pH 3.0) containing 20 µM $HgCl_2$ solution at bare GCE, HA and Av-HA modified glassy carbon electrodes at the scan rate of 50 mVs^{-1}. A well defined oxidation peak is observed at 0.24 V corresponding to oxidation of metallic mercury ($Hg^0 \rightarrow Hg^{2+} + 2e^-$). It may be noticed that the potential window was chosen in the range of -0.8 to 0.6 V. The peak

current (i_{pa}) values of bare GCE, HA and Av-HA modified electrodes were found to be 1.52 μA, 2.75 μA and 4.24 μA respectively. The Av-HA modified GCE shows higher anodic peak current when compared to bare GCE and HA modified GCE which clearly demonstrate that Av-HA modified GCE has improved electrochemical activity than the HA modified GCE. Fig. 5B shows the comparison of mercury detection characteristics of bare GCE, pristine HA and Av-HA modified GCE investigated using square wave voltammetry (SWV) in 0.2 M KNO_3 (pH 3.0) containing 20 $x10^{-6}$ M $HgCl_2$ solution. The Av-HA/GCE showed a well defined sharp peak (i_{pa}=5.2 μA) which is 2 and 1.5 times higher than that of bare GCE (i_{pa}=2.6 μA) and pristine HA (i_{pa}=3.3 μA) modified GCE respectively.

<Fig. 5>

In most of the heavy metal ion sensors, the target metal ion (Hg^{2+}) get adsorbed on the modified electrodes (eqn.1) during the course of pre-deposition treatment and subsequently it undergoes oxidation (eqn.2). Interestingly, the Av-HA modified GCE does not require any pre-accumulation for the oxidation of mercury when compared to the literature reports [3-8]. In order to optimize the initial potential required for pre-deposition free CV and SWV measurements, a systematic study was carried out at various initial scan potential (0, -0.2, -0.4,-0.6, -0.8, -1.0 and -1.2 V) towards the oxidation of mercury at Av-HA/GCE in 0.2 M KNO_3 (pH 3.0) containing 20 μM $HgCl_2$ solution and the results are shown in Fig. 6A.

$$Hg^{2+} + 2^{e-} \rightarrow Hg^0 \qquad (1)$$

$$Hg^0 \rightarrow Hg^{2+} + 2^{e-} \qquad (2)$$

The scan potential of -0.8 V shows the highest peak current when compared to the other scanning potentials. Here, a partial accumulation of Hg^0 takes place during the scan from -0.8 V till the oxidation peak potential (0.24 V). This enables the determination of mercury ions without requiring preconcentration step. Hence we have used -0.8 V as initial scan potential for further experiments.

Mercury (Hg^{2+}) ions have different electrochemical behaviours in different electrolytes. The effects of electrolytes, such as HCl, phosphate buffer, acetate buffer, and KNO_3, on oxidation peak currents of Hg^{2+} were studied and the results have shown that the Hg^{2+} ions have the best electrochemical responses in 0.2 M KNO_3. When the measurements were performed in this electrolyte well defined peaks with the lowest background current were obtained.

The influence of pH on the oxidation of mercury at the Av-HA modified glassy carbon electrode in 0.2 M KNO_3 containing 20 μM $HgCl_2$ solution was also investigated by CV studies (Fig. 6B). The anodic peak current is strongly dependent on the pH of the solution with the maximum being was observed at pH 3.0. At higher pH values (>5.0), the peak current decreased rapidly and the peak shape was also destroyed which could be attributed to the hydrolysis of Hg^{2+}. Similarly, CV measurements at lower pH values (< 3.0) yield lower oxidation current due to the dissolution of hydroxyapatite in high acidic medium. Based on these observations, pH 3.0 was chosen as the optimum value for the supporting electrolyte.

<Fig. 6>

3.5 Determination of Hg^{2+} by square wave voltammetry

Square wave voltammetry (SWV) was used to examine the sensitivity of Av-HA/GCE towards the detection of mercury (II) ions. Fig. 7 shows the SWV response of the Av-HA/GCE to the successive addition of mercury in 0.2 M KNO_3 (pH 3.0). The Av-HA/GCE exhibited a rapid and sensitive response to the change of mercury concentration and an obvious increase in anodic peak current upon successive addition of mercury. Further, current was increased linearly with increasing Hg^{2+} concentration in the range of 2.0×10^{-7} to 2.1×10^{-4} M (inset of Fig. 7) and the detection limit was found to be 141 nM with a correlation coefficient of 0.993. The present experiments demonstrated that it is possible to determine Hg^{2+} using Av-HA modified GCE without fouling of the electrode surface for

repeated measurements. These results confirmed that Av-HA modified electrode provide a good electrocatalytic platform toward mercury sensing.

<Fig. 7>

3.6 Interference study

Selectivity of the modified Av-HA/GCE was evaluated by introducing different solutions of other metal ions (20 μM of Cd^{2+}, Pb^{2+}, Cu^{2+}, Zn^{2+}, Ag^{+}) and 20 μM of Hg^{2+}) in 0.2 M KNO_3 solution of pH(3.0). The cyclic voltammograms (Fig. 8A) shows one oxidation signal corresponding to Hg^{2+} at 0.204 V and three clear peaks corresponding to potential interferents Cd^{2+}, Pb^{2+} and Cu^{2+}. A clear separation of various peaks offers the possibility of the determination of Hg^{2+} without any effective interference from the investigated interferents. Ag^{+} and Zn^{2+} did not affect the oxidation peak current of Hg^{2+}. Copper can be expected to be a major interferent in the detection of mercury as its oxidation potential is close to that of mercury. To examine the analytical performance of the Av-HA modified GCE towards the detection of Hg^{2+} in the presence of Cu^{2+}, SWV measurements have been performed in the presence of 20 μM Cu^{2+} in 0.2 M KNO_3 of pH 3.0 (Fig. 8B). As can be seen, two distinct anodic peaks appear for Hg^{2+} and Cu^{2+} with a separation potential of 0.1 V and a very clear signal could be observed for 0.1 μM mercury in the presence of 20 μM copper, which revealed that the detection of very low concentration of mercury is possible even in the presence of 20 times of copper. The result indicates that the selective determination of mercury is possible using the fabricated sensor.

<Fig. 8>

3.7 Stability and reproducibility of Av-HA/GCE electrode

In order to investigate the stability of the Av-HA/GCE electrode, the cyclic voltammogram current responses for 20 μM mercury in 0.2 M KNO_3 (pH 3.0) was recorded for every 2 h interval over a period of 24 hours. It was found that the oxidation current

remained nearly the same with a relative standard deviation of 4.67%. To further establish the reproducibility of the experimental results, four different Av-HA modified electrodes were tested towards the detection of 20 μM mercury in 0.2 M KNO_3. The CV current obtained by the four independent electrodes showed a relative standard deviation of 3.5% for mercury, confirming that the sensor is reproducible. These results indicate that the Av-HA modified electrode has good stability, reproducibility and does not undergo surface fouling. The main features of the newly fabricated mercury sensor are that the sensing material hydroxyapatite was prepared through biosynthesis procedure in presence of *Aloe vera* plant extract and that the electrode modification procedure adopted was the simple drop casting method. Most importantly, no accumulation time is needed for the detection of Hg^{2+} at the Av-HA modified glassy carbon electrode when compared to the literature reports (Table 1).

<Table 1>

3.8 Analytical applications

In order to evaluate the applicability of the proposed Av-HA NPs modified GCE for the determination of Hg^{2+} in real samples, its utility was tested by determining the mercury ion in tap water and industry waste water. Samples were collected from distillery industry near Sivaganga town. The water samples were used without pretreatment and the pH value was adjusted to 3.0 with hydrochloric acid. Satisfactory recovery was found for mercury detection (Table 2). The results show that the fabricated sensor has potential for applications in the determination of mercury in real samples.

<Table 2>

4. Conclusions

We have demonstrated the synthesis of *Aloe vera* assisted hydroxyapatite nanoparticles by an environment friendly approach and its application in direct voltammetric determination of mercury (II) ions. The Av-HA modified GCE exhibited improved electrocatalytic activity toward the oxidation of mercury and it does not require any preconcentration treatment. The linear range and the lowest detection limit for the fabricated mercury electrochemical sensor were found to be 2.0×10^{-7} to 2.1×10^{-4} M of Hg^{2+} and 141 nM respectively. The Av-HA modified electrode showed good selectivity towards the determination of mercury in the presence of potential interferents such as copper, lead, cadmium, silver and zinc. High stability and reproducibility make the proposed HA modified GCE to be very useful for accurate determination of mercury. Further, the Av-HA/GCE fabrication is very simple and inexpensive and this sensor will be useful for mercury detection in environmental, food or pharmaceutical samples.

Acknowledgement

One of the authors (P.K) acknowledges with thanks the University Grants Commission (UGC), India for providing the Post Doctoral Fellowship (No. F.15-1/2011-12/PDFWM-2011-12-OB-TAM-2867 (SA-II)). C.S acknowledges the CSIR for funding (F.No. 03 (1203)/12/EMR-II).

References

1. N.L. Dias, D.R. Do Carmo, L. Caetano, A.H. Rosa, Anal. Sci., 21 (2005) 1359–1363.
2. I. Onyido, A. R. Norris, E. Buncel, Chem. Rev. 104 (2004) 5911–5929.
3. S. Anandhakumar, J. Mathiyarasu, K. L. N. Phani, Anal. Methods 4 (2012) 2486–2489.
4. L.H. Marcolino-Junior, B.C. Janegitz, B.C. Lourenção, O. Fatibello-Filho, Anal. Lett. 40 (2007) 3119–3128.
5. Hongchao Yi, Anal. Bioanal. Chem. 377 (2003) 770–774.
6. O. Abollino, A. Giacomino, M. Malandrino, G. Piscionieri, E. Mentasti, Electroanal. 20 (2008) 75 – 83.
7. Q.X. Zhang, D. Peng, X. Jiu Huang, Electrochem. Commun. 34 (2013) 270–273.
8. Gabriela Roa-Morales, M. T. Ramrez-Silva, Rosendo Lopez Gonzalez, Laura Galicia, M. Romero-Romo, Electroanal. 17 (2005) 694-700.
9. O. Ordeig, C.E. Banks, J. Del Campo, F.X. Munoz, R.G. Compton, Electroanalysis, 18 (2006) 573.
10. C. Welch, O. Nekrassova, X. Dai, M. Hyde, R.G. Compton, Chem Phys Chem., 5 (2004) 1405.
11. K.Z. Brainnina, N.Y. Stozhko, J. Shalygina, Anal Chem., 59 (2004) 753.
12. M.A. El Mhammedi, M. Achak, M. Bakasse, Arab.J. Chem. 6 (2013) 299-305.
13. K. Mori, K. Yamaguchi, T. Hara, T. Mizugaki, K. Ebitani, K. Kaneda, J. Am. Chem. Soc. 124 (2002) 11572.
14. P. Kanchana, N. Lavanya, C. Sekar, Mater. Sci. Eng. 35 (2014) 85-91.
15. P. Kanchana, C. Sekar, Mater. Sci. Eng. 42 (2014) 601-607.
16. P. Kanchana, C. Sekar, Spectrochim. Acta. A 137 (2015) 58-65.
17. D.W. Hess, K.F. Jensen, T.J. Anderson, Rev. Chem. Eng. 3 (1985) 130.
18. M.D. Boudreau, F.A. Beland, J. Environ. Sci. Health C 24 (2006) 103–154.
19. S.P. Chandran, M. Chadudhary, R. Pasricha, A. Ahamad, M. Sastry, Biotechnol. Progr. 22 (2006) 577-583.
20. S. Koutsopoulos, J. Biomed. Mater. Res. 62 (2002) 600–612.
21. S. Shiv Shankar, Absar Ahmad, Murali Sastry, Biotechnol. Progr. 19 (2003) 1627-1631.

22. X. Liu, C. Sun, H. Wu, Y. Zhang, J. Jiang, G. Shen, R. Yu, Electroanal. 22 (2010) 2110 – 2116.

23. F. El Aroui , S. Lahrich , A. Farahi , M. Achak , L. El Gaini , B. Manoun , M. Bakasse, A. Bouzidi, M.A. El Mhammedi, J.Taiwan Inst. Chem.Eng. 45(2014)2615-2621.

24. Z.Q. Zhao, X. Chen, Q. Yang, J.H. Liua, X.J. Huang, Chem. Commun. 48 (2012) 2180–2182.

Figure captions

Fig. 1(A) XRD pattern of a) pristine HA and b) Av-HA nanoparticles; (B) FT-IR spectra of a) pristine HA and b) Av-HA

Fig. 2 FE-SEM images and EDX spectra of pristine HA (a,c) and Av-HA (b,d).

Fig. 3 TEM images of Av-HA at different magnifications

Fig. 4 TG curves of pristine HA and Av-HA nanoparticles

Fig. 5 (A) Cyclic voltammograms of a) bare GCE, b) HA and c) Av-HA modified GCE recorded in 0.2 M KNO_3 (pH 3.0) containing 20 μM Hg^{2+} at the scan rate 50 mVs^{-1}; (B) Square wave voltammograms of a) bare GCE, b) HA and c) Av-HA modified GCE recorded in 0.2 M KNO_3 (pH 3.0) containing 20 μM Hg^{2+}; amplitude 50 mV; step potential 0.05 V.

Fig. 6 (A) Influence of initial scan potential (0, -0.2, -0.4,-0.6, -0.8, -1.0 and -1.2 V) on cyclic voltammogram response towards the oxidation of 20 μM Hg^{2+} in 0.2 M KNO_3 (pH 3.0) at Av-HA/GCE at the scan rate 50 mVs^{-1}; (B) Effect of pH on CV peak currents of 20 μM Hg^{2+} in 0.2 M KNO_3 at Av-HA modified GCE at the scan rate 50 mVs^{-1}.

Fig. 7 SWVs of the Av-HA modified GCE in 0.2 M KNO_3 (pH 3.0) with various concentration of Hg^{2+}; amplitude 50 mV; step potential 0.05 V. The concentration of Hg^{2+} was varied from 0.2 to 210 μM. Inset shows the calibration plot of SWV response.

Fig. 8 (A) Cyclic voltammogram of 20 μM each Hg^{2+}, Cd^{2+}, Pb^{2+} and Cu^{2+} in 0.2 M KNO_3 (pH 3.0) at Av-HA modified GCE recorded at the scan rate of 50 mVs^{-1}; (B) SWVs for various concentrations of Hg^{2+} (0.1-100 μM) in presence of 20 μM Cu^{2+} recorded using Av-HA/GCE in 0.2 M KNO_3 (pH 3.0) under amplitude 50 mV and step potential 0.05 V.

Table caption

Table 1 Comparison of different chemically modified electrodes for the determination of Hg^{2+} with Av-HA/GCE

Table 2 Determination of Hg^{2+} at various concentrations in tap water and industry waste water

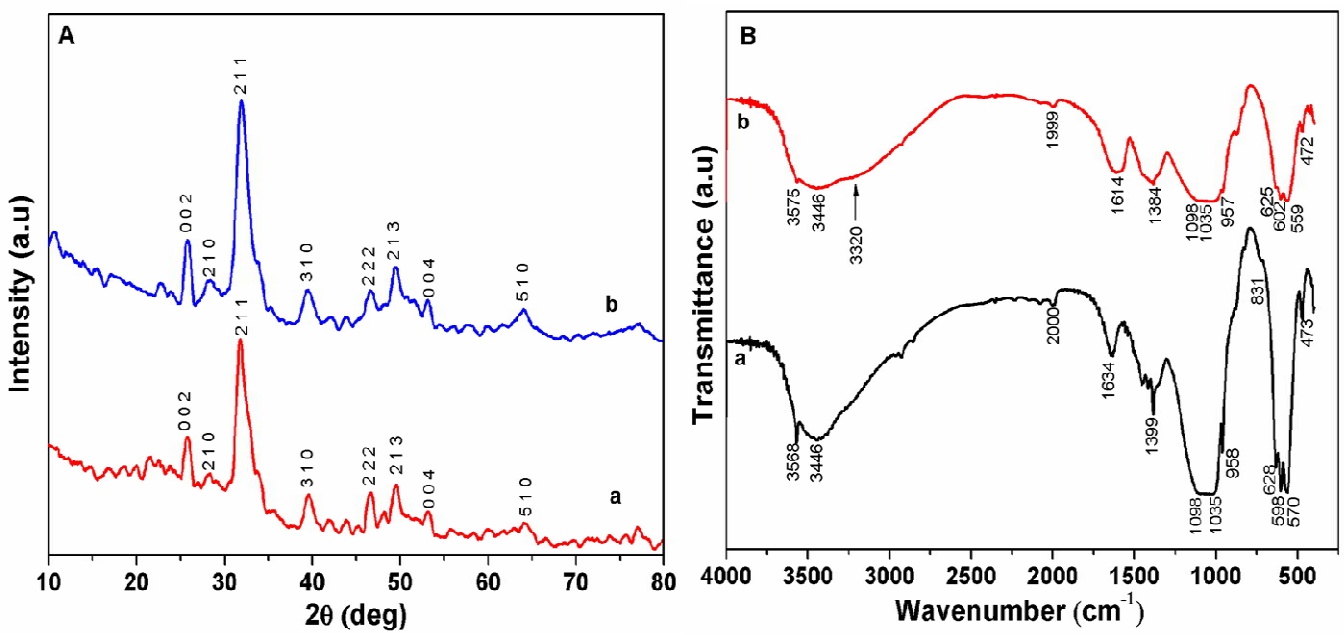

Fig. 1

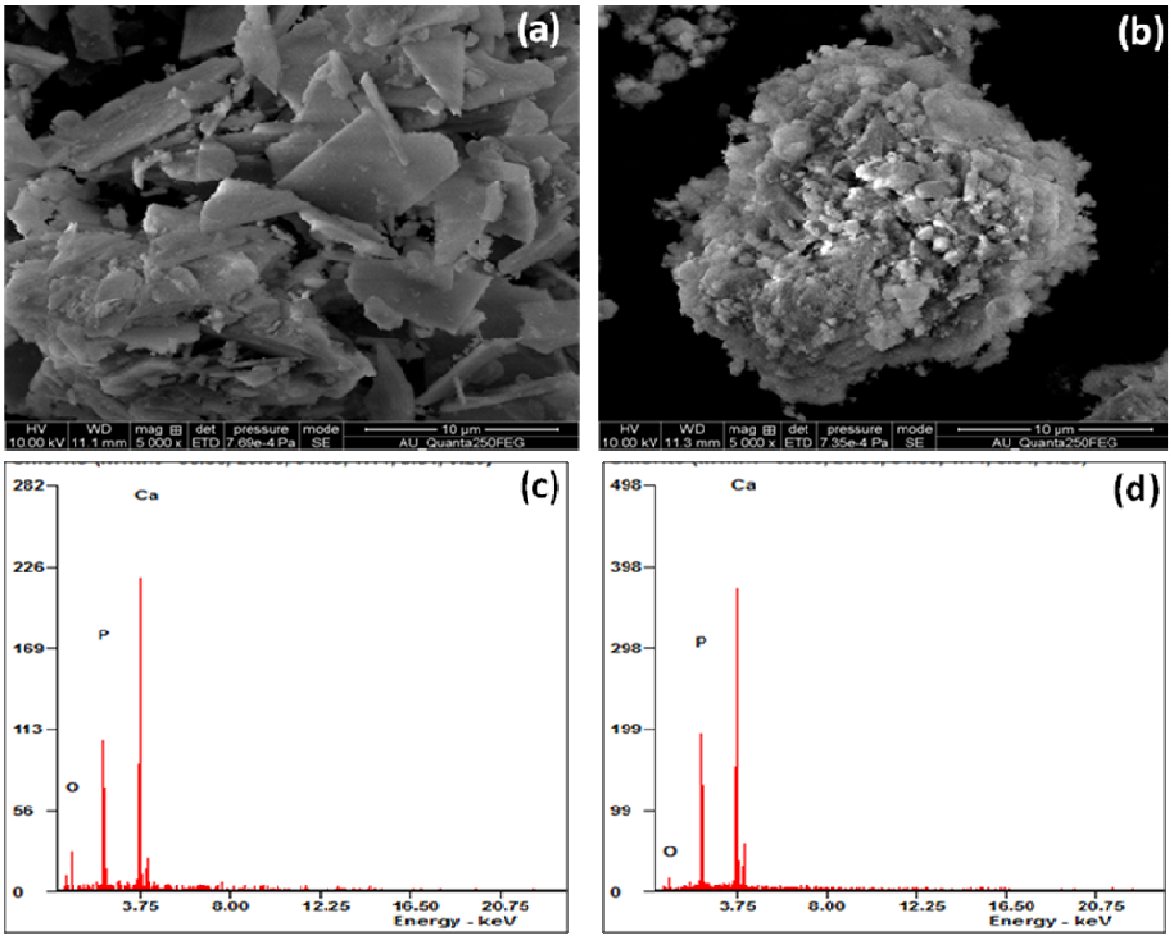

Fig. 2

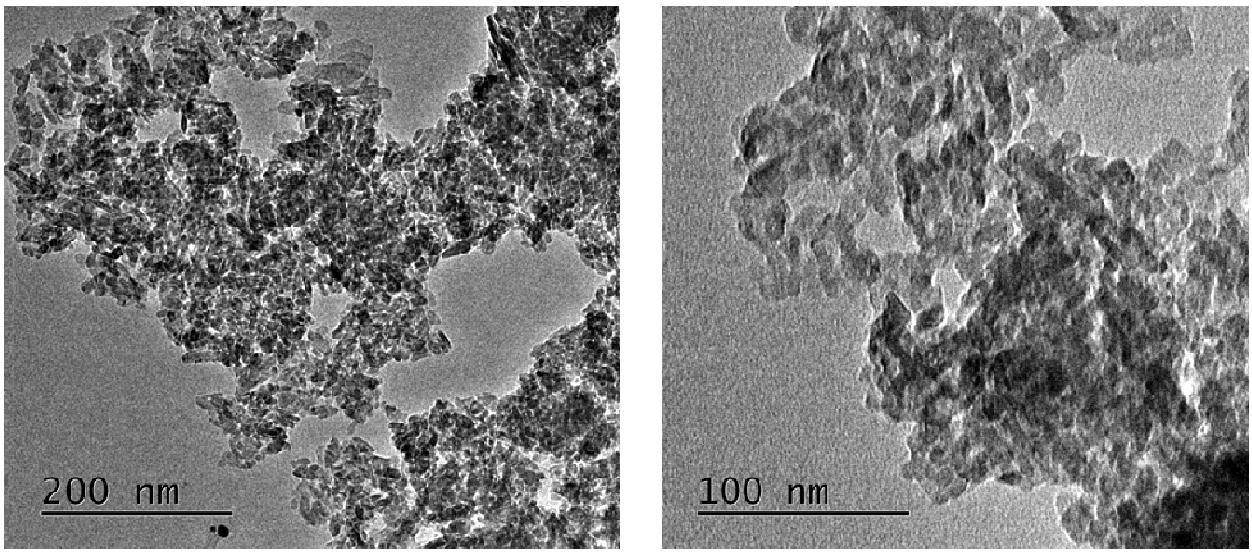

Fig. 3

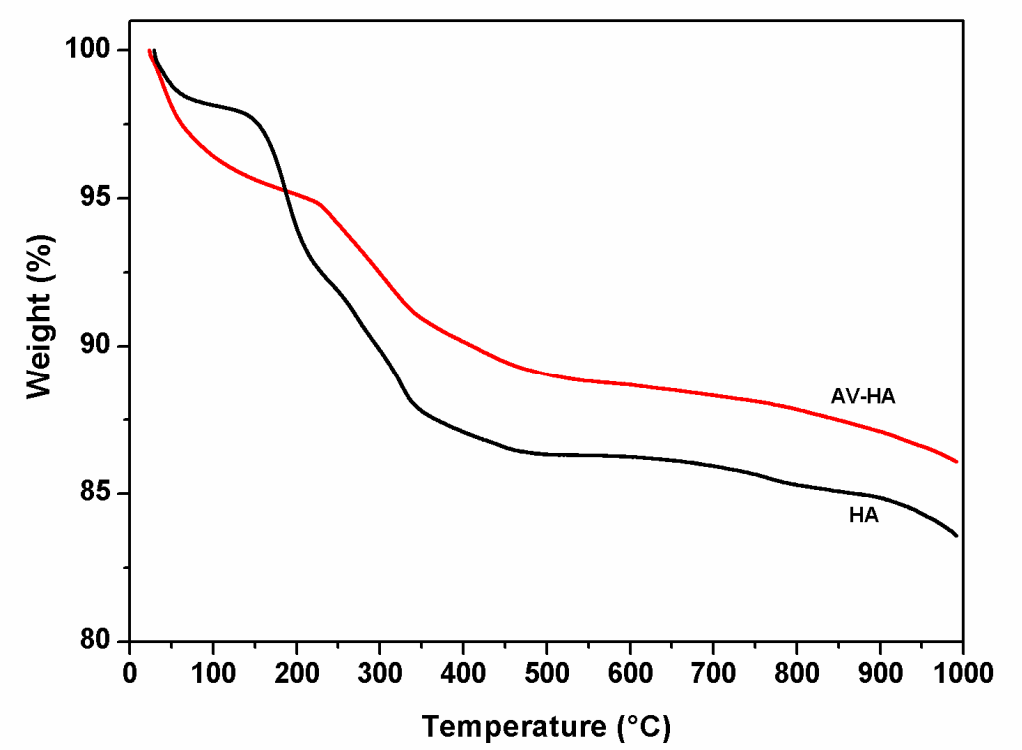

Fig. 4

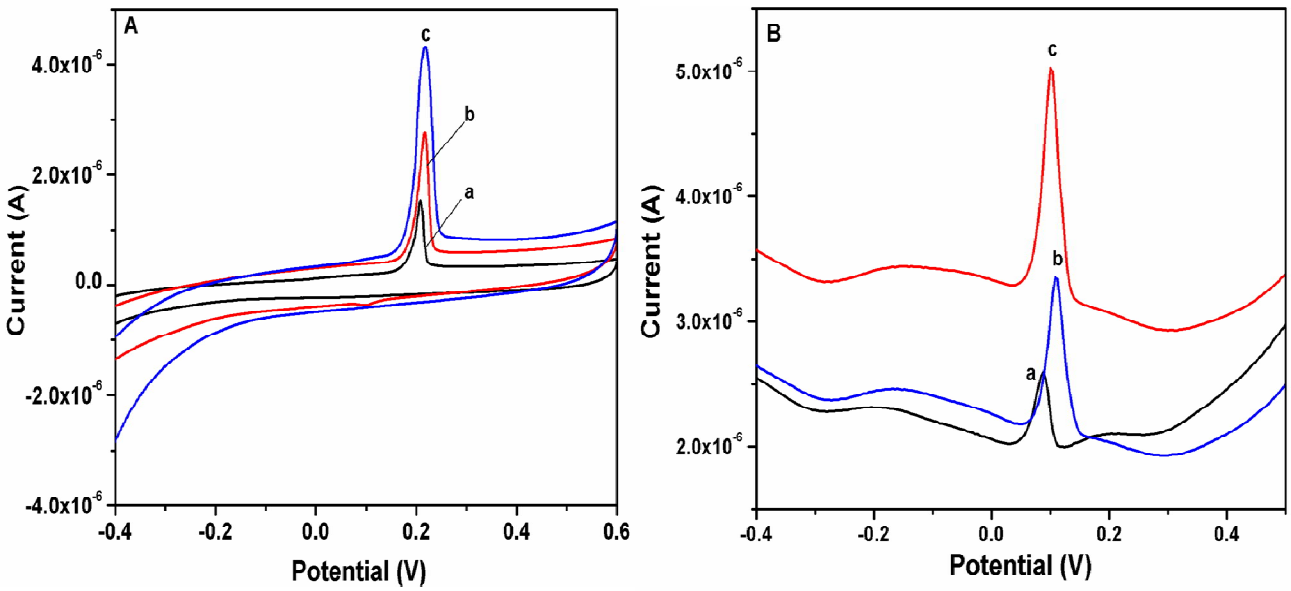

Fig. 5

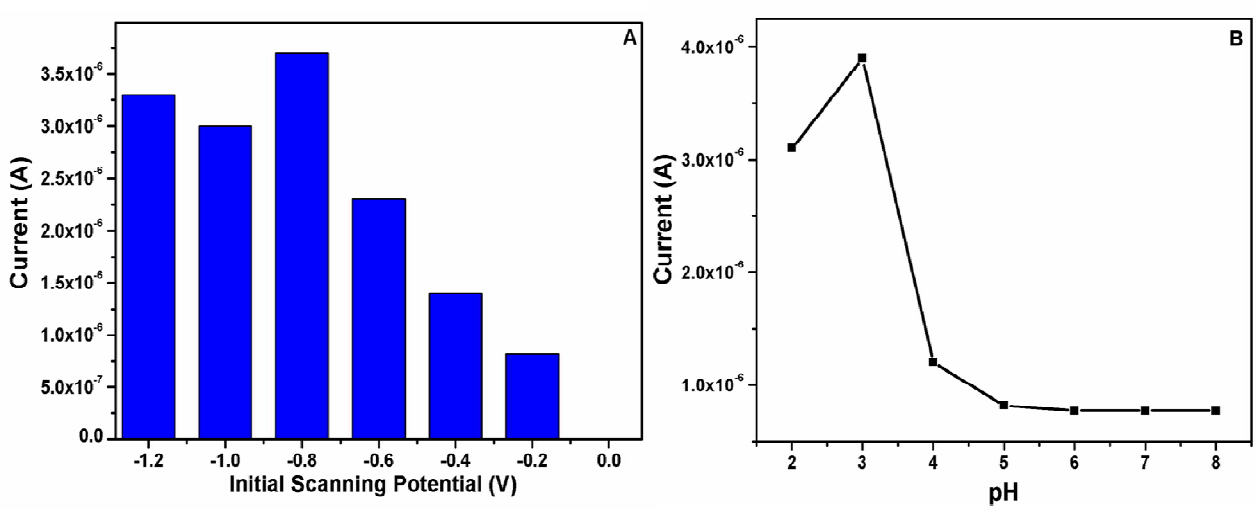

Fig. 6

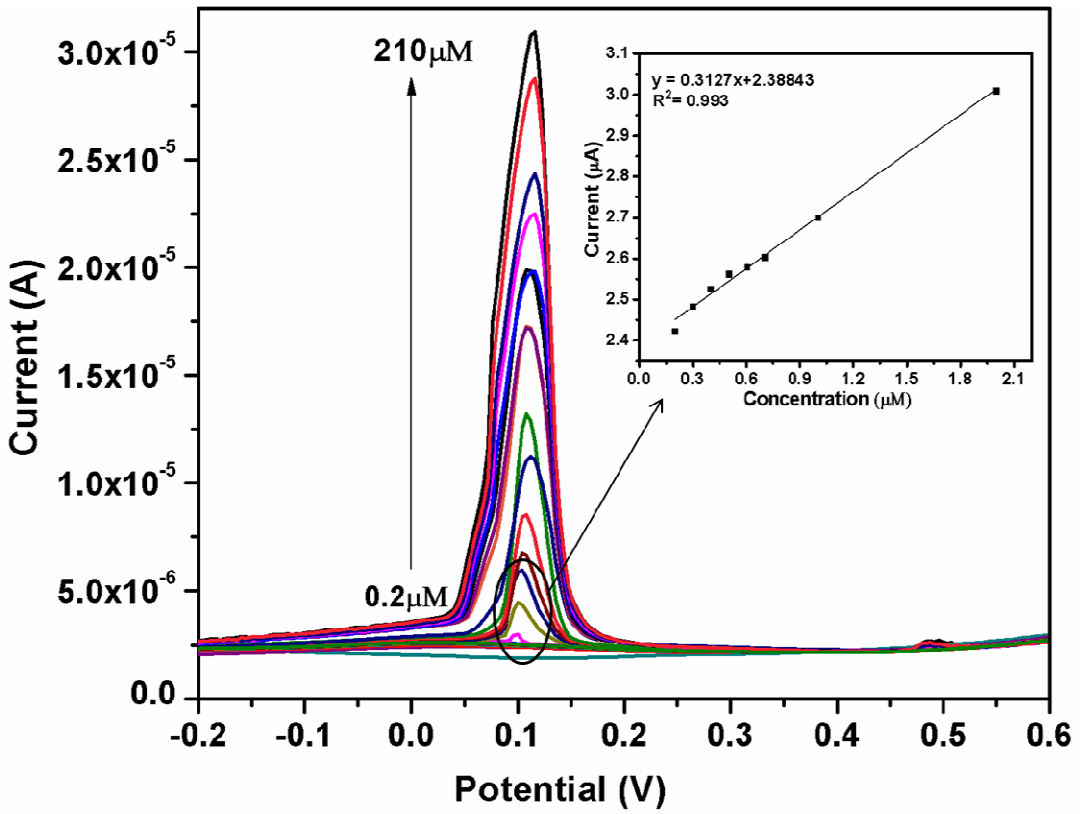

Fig. 7

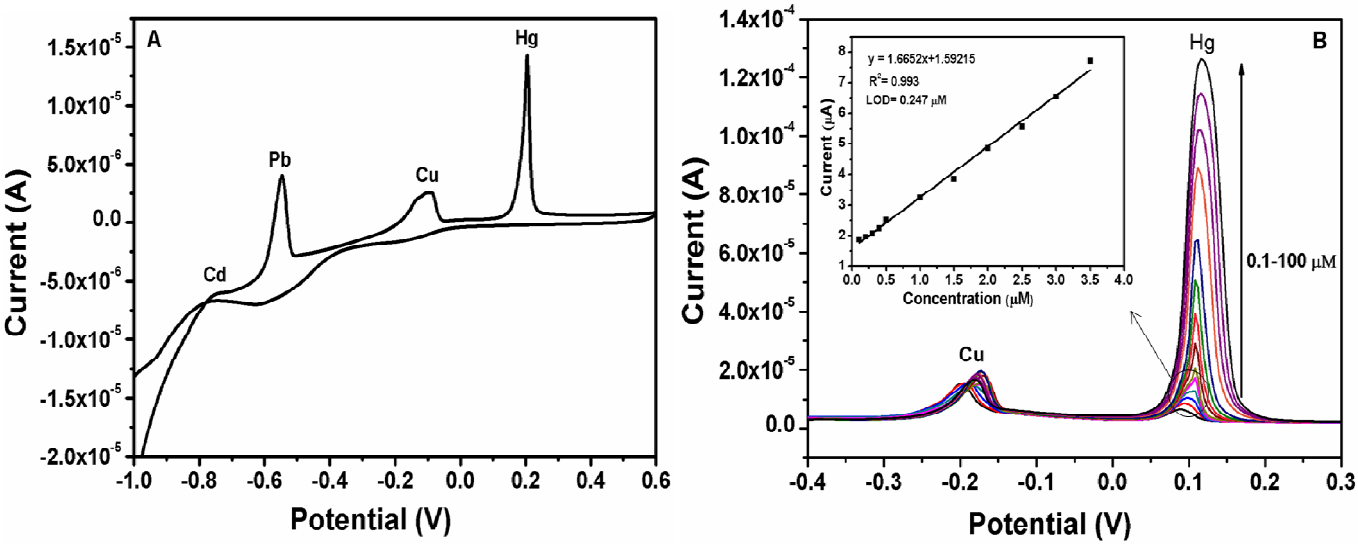

Fig. 8

Table 1 Comparison of different chemically modified electrodes for the determination of Hg^{2+} with Av-HA/GCE

Electrode	Method	Linear range (μM)	Detection limit (nM)	References
Au-PEDOT/ GCE	SWASV	10-70	5000	[3]
Chitosan/ CPE	ASV	0.9 –38.5	628	[4]
MWCNT/GCE	ASV	0.00008–0.5	0.2	[5]
nanoAu/HDT/GE	DPV	0.001-0.5	0.32	[22]
PdO/NP-CPE	DPASV	0.25-150	19.3	[23]
PPy–RGO/GCE	SWASV	0-0.1	15	[24]
Av-HA/GCE	SWV	0.2- 210	141	Present work

Table 2 Determination of Hg^{2+} at various concentrations in tap water and industry waste water

Sample	Added (μM)	Found (μM)	Recovery (%) (n=3)
Tap water	5	4.85	97
	10	10.1	100
	15	14.25	95
Industry waste water	5	5.09	101.8
	10	10.24	102.4
	15	14.96	99.73

Graphical Abstract